Inhibition of phosphatidylinositol-3-kinase synergizes with gemcitabine in low-passage tumor cell lines correlating with Bax translocation to the mitochondria

Carmen Blanco-Aparicio[a], Belen Pequeño[a], Victoria Moneo[a], Lourdes Romero[a], Juan F. M. Leal[a], Juan Velasco[b], Jesús Fominaya[a] and Amancio Carnero[a]

Apoptotic pathways, including the phosphatidylinositol-3-kinase (PI3K)/AKT survival pathway, are altered in most cancer cells in relation to their normal counterparts and these differences may present an excellent therapeutic window. To gain insight into the relevance of the PI3K pathway as a target for drug discovery we generated tumor cell lines from different tumor samples that we maintained at low passage. The characterization of these cell lines indicates that all of them have constitutively activated the PI3K pathway through different mechanisms. All cell lines were differentially sensitive to the PI3K inhibitor LY294002. Our data also support previous work indicating that PI3K inhibition might help classical chemotherapeutic treatments such as gemcitabine and strengthen suboptimal doses that might be effective for these purposes in decreasing the risk of side-effects. Finally, the analysis of the molecular markers that might be implicated in the synergism between LY294002 and gemcitabine suggests that PI3K inhibition might aid chemotherapeutic treatment, leading to changes in the balance between anti- and pro-apoptotic molecules of the Bcl-2 family, Bcl-X_L and Bax. These results facilitate the exploration of potential synergism between chemotherapeutic treatment and the search for others that can account for similar molecular mechanisms of cooperation. ***Anti-Cancer Drugs*** **16:977–987**

Anti-Cancer Drugs 2005, **16**:977–987

Keywords: AKT, Bax, Bcl-X_L, gemcitabine, pharmacological synergism, phosphatidylinositol-3-kinase

[a]Experimental Therapeutics Programme, Spanish National Cancer Center (CNIO), Madrid, Spain and [b]Lilly Research Laboratories, Alcobendas, Madrid, Spain.

Sponsorship: This work was supported in part by the Spanish MCyT (project BIO2001-0069) and FIS (project FIS-02/0126).

Correspondence to A. Carnero, Experimental Therapeutics Programme, Spanish National Cancer Center (CNIO), c/Melchor Fernandez Almagro no. 3, 28029 Madrid, Spain.
Tel: +34 91 732 8021; fax: +34 91 224 6976;
e-mail: acarnero@cnio.es

Received 19 April 2005 **Revised form accepted** 8 July 2005

Introduction

Several signaling pathways have been shown to impact the apoptotic potential of cells, most notably the phosphatidylinositol-3-kinase (PI3K)/AKT pathway (also called the survival pathway) [1]. The serine/threonine kinase AKT is a major downstream target of growth factor receptor tyrosine kinases that signal via class 1A PI3K. These enzymes are heterodimers that consist of a catalytic subunit of relative molecular mass 110 kDa (p110α, β or δ) in complex with an adapter molecule (p85) with SH2 domains. PI3K may also directly interact and be activated by oncogenic Ras [2,3]. Thus, through several possible protein–protein interaction-activated growth factor receptors PI3K is recruited to the membrane where the PI3K p110 subunit phosphorylates membrane phosphoinositides at the D-3 position. The N-terminus of AKT contains a pleckstrin homology domain that is thought to directly bind the phospholipid products of PI3K. This binding recruits AKT to the membrane, and induces a conformational change that allows the phosphorylation of AKT by the phosphoinositide-dependent kinases (PDK) I and II at residues Thr308 and Ser473, respectively. The phosphorylation at Thr308 is necessary for AKT activation, whereas Ser473 phosphorylation is only required for maximal activity. AKT has been documented to phosphorylate and inactivate multiple substrates relevant to apoptosis, including the Bcl-2 family member Bad, caspase-9, forkhead transcription factors, Bax and YAP [4].

Survival factors suppress intrinsic cell death machinery and thereby prevent apoptosis. The PI3K/AKT pathway is a general mediator of growth factor-induced survival and has been shown to suppress the apoptotic death of a number of cell types induced by a variety of stimuli, including c-*myc* overexpression, growth factor withdrawal, cell cycle deregulation, loss of cell adhesion and DNA damage [4–6]. Conversely, inhibition of PI3K/AKT signaling sensitizes cells to apoptotic stimuli. Expression of a dominant-negative AKT mutant accelerates cell death upon serum deprivation or differentiation [7,8].

Consistent with these data, human cancer cell lines lacking active lipid phosphatase PTEN have been shown to be less sensitive to apoptotic stimuli than cells from the same cancer type with normal PTEN function [9,10].

0959-4973

Furthermore, cells exhibiting increased signaling through the PI3K/AKT pathway have been shown as more sensitive to PI3K inhibition by LY294002 [11,12]. This difference may be exploited therapeutically.

Collectively, these data suggest that any compound with the ability to decrease overstimulated PI3K/AKT signaling should increase apoptosis. Although activation of apoptotic pathways leads to the death of untransformed cells, a fundamental difference exists between tumor cells and their normal counterparts, as normal cells neither have to sustain the pro-apoptotic onslaught inherent to deregulated proliferation nor survive away from their usual environment in the absence of requisite survival signals. Repair or replacement of relevant apoptotic signaling components could well prove too much for a tumor cell already burdened with a heavy apoptotic load. In the present work we have generated and characterized low-passage cell lines from primary oncogenic tissue. We have characterized these cell lines for PI3K pathway activation, and studied *in vitro* and *in vivo* whether inhibition of PI3K is a suitable pharmacological approach either alone or in combination with gemcitabine. We also analyzed the molecular determinants of such synergism.

Materials and methods

Generation of cell lines and culture conditions

Sterile fragments from the resected tumor were minced in culture medium and then disaggregated by 1–2 h incubation in collagenase (100 U/ml) at 37°C. After 24 h the medium was changed to F-10 Ham (Gibco, Carlsbad, California, USA) supplemented with 1% Ultroser G (Biosepra, Fermont, California, USA). Cell lines generated were cultured in F-10 Ham supplemented with 10% FBS, 1% Ultroser and antibiotics (100 U/ml penicillin/100 μg/ml streptomycin).

To subculture the cell lines, once cells became confluent, adherent cells were detached by trypsin–EDTA treatment and replated at a 1:2 or 1:3 ratio with fresh medium. Phenotypic features were followed throughout the establishment of these cell lines. Additionally, they were routinely examined for mycoplasma contamination (InvivoGen, San Diego, California, USA). Cells were used in the exponential growth phase for all the experiments.

Drugs

LY294002 and gemcitabine (2′,2′-difluorodeoxycytidine) were supplied by Lilly (Indianapolis, Indiana, USA). Gemcitabine was diluted in sterile water at a concentration of 100 μM and LY294002 was diluted in DMSO at a concentration of 100 mM. The drugs were freshly diluted in culture medium before each experiment, at a final concentration below 1% DMSO, with appropriate solvent additions to control cultures.

Assessment of cytotoxicity

The compounds were tested on 96-well plates. Cells growing in a flask were harvested just before confluence, counted using a hemocytometer and diluted with media to adjust the density to 4000 cells/well. The cells were allowed to sit and grow for 24 h before adding the drugs.

A 'mother plate' with serial dilutions was prepared at 200 times the final concentration in the culture from the compounds diluted to a concentration of 100 mM. DMSO in the culture media did not exceed 0.5%. The appropriate volume of the compound solution (usually 2 μl) was then automatically added (FX 96 tip; Beckman, Fullerton, California, USA) to the culture media.

Old media were then removed from the cells and replaced with 0.2 ml of media dosed with drug. Each concentration was assayed in triplicate. Two sets of control wells were left on each plate, containing either medium without drug or medium with the same concentration of DMSO. A third control set was obtained with the cells untreated just before adding the drugs (seeding control, number of cells starting the culture).

Cells were exposed to the drugs for 96 or 120 h in the case of LY294002 and gemcitabine, respectively, and then washed twice with phosphate-buffered saline before being fixed with 0.5% glutaraldehyde. Cells were washed twice and stained with 1% crystal violet for 30 min. Finally they were washed extensively, solubilized with 15% acetic acid and quantitated by measuring the absorbance at 595 nm by means of a microplate reader (Bio-Rad, Hercules, California, USA).

Single-drug exposure

In the cytotoxicity assay, LY294002 and gemcitabine were tested singly at scalar concentrations of 0.017, 0.051, 0.15, 0.46, 1.37, 4.12, 12.35, 37.04, 111.11, 333.33 and 1000 μM for LY294402 and 0.017, 0.051, 0.15, 0.46, 1.37, 4.12, 12.35, 37.04, 111.11, 333.33 and 1000 nM for gemcitabine. For LY294402, the treatment medium was changed every day by adding fresh LY294002 and an exposure time of 96 h was selected from the dose–survival curves. In the case of gemcitabine, the medium was changed by adding fresh gemcitabine 48 h after the first addition and an exposure time of 120 h was chosen from the dose–survival curve.

Drug combination

Gemcitabine and LY294002 were added simultaneously, and the exposure was 120 h, following the protocol described for gemcitabine alone. In combination experiments gemcitabine was tested at the different concentrations used for single-drug exposure, and LY294002 was added at a ratio 1:1 at 0.1, 10 and 40 μmol/L.

Drug interaction analysis

We used Kern's method [13], subsequently modified by Romanelli [14]. In short, the expected cell survival S_{exp}, defined as the product of the survival observed with drug A alone and the survival observed with drug B alone, and the observed cell survival (S_{obs}) for the combination of A and B were used to construct an index (RI): $RI = S_{exp}/S_{obs}$. $RI \leq 1$ indicates the absence of synergism or antagonism. Synergism was defined as any value of $RI > 2$. $1 \leq RI \leq 2$ indicates additive effects.

Western blot analysis

Cells grown in 10% FBS medium were serum starved (0.5% FBS) 24 h before obtaining the lysates, and were treated with LY294002 10 μmol/L for 1 h before harvesting AKT or FKHRL-1 phosphorylation was used as the endpoint of PI3K activation. Cells were also treated with LY294402 10 μmol/L, gemcitabine 100 nmol/L or both drugs for 24 h before harvest, and Bax and Bcl-X_L were used as the endpoint of apoptosis induction. Cells (1×10^6) were washed twice in ice-cold PBS and then incubated with 1 ml of lysis buffer (1% NP-40, 50 mmol/L Tris–HCl, pH 7.4, 150 mmol/L NaCl, 1 mmol/L Na_3VO_4, 20 mmol/L $Na_4P_2O_7$ and 100 mmol/L NaF) and complete protease inhibitor cocktail tablet (Roche Molecular Biochemicals, Mannheim, Germany, Spain) for 5 min on ice. Whole-cell lysates were clarified by centrifugation at 15 000 r.p.m. for 10 min at 4°C, Protein concentration was determined with a Bradford reagent (Bio-Rad, California, USA). Samples (10 μg of each lysate) were heated in SDS sample buffer for 5 min at 95°C, run on 10% SDS–polyacrylamide gels and transferred to PVDF membranes (Millipore, Billerica, Massachusetts, USA) using the Mini Trans-Blot electrophoresis transfer cell (Bio-Rad). Membranes were blocked for 4 h with 1% BSA in TBST (10 mM Tris, pH 7.6, 150 mM NaCl and 0.5% Tween-20) and then exposed to a primary antibody specific for AKT phosphorylated at S473 (New England Biolab, Beverly, Massachusetts, USA), AKT (New England Biolab), PTEN (Cascade, Wenham, Massachusetts, USA), p110α (Upstate Biotechnology, Lake Placid, New York, USA), p53 (FL-393; Santa Cruz Biotechnology, Santa Cruz California, USA) and Bcl-X_L (Dako, Denmark) overnight at 4°C in the same blocking solution. The membrane was then washed and incubated for 45 min with secondary antibody containing horseradish peroxidase (anti-mouse IgG; Promega, Madison, Wisconsin, USA) or anti-rabbit IgG (Calbiochem, San Diego California, USA), and developed with a detection system for chemiluminescence (Amersham Biosciences, Little Chalfont, UK).

RT-PCR

Total RNA was purified using the TRI-REAGENT (Molecular Research Center, Cincinnati Ohio). Reverse transcription was performed with 1 μg of Rnasy (Promega) following the manufacturer's protocol. The following primers were used to amplify regions: p73α forward 5′-TTTAACAGGATTGGGGTGTCC-3′ and reverse 5′-CGTGAACTCCTCCTTGATGG-3′; β-actin, forward 5′-AGGCCAACCGCGAGAAGATGAC-3′ and reverse 5′-GA AGTCCAGGGCGACGTAGCA-3′. CDNA was subjected to PCR and products were analyzed by 1% agarose gel electrophoresis.

Immunostaining and confocal analysis

Cells were seeded at 1×10^4 cells/cm^2 onto glass coverslips and cultured for 24 h; the cells were then treated with 10 μmol/L LY294002, 100 nmol/L gemcitabine or a combination of both drugs in vehicle (DMSO). After 24 h, cells were incubated with 75 nmol/L Mitotracker Red CMXRos for 45 min at 37°C and washed with PBS. Coverslips were fixed in 2% paraformaldehyde for 15 min at room temperature and washed 5 times in PBS. Samples were incubated in blocking solution (PBS containing 3% BSA) at room temperature for 15 min, followed by incubation overnight at 4°C with anti-Bax antibody. After washing with PBS, cells were incubated with species-specific Alexa 633-conjugated secondary antibody diluted 1:200 in blocking buffer for 1 h at room temperature in the dark. The nuclei were stained with Hoechst 33258 for 10 min at room temperature in the dark prior to mounting with fluoromount (Dako). Images were collected by confocal laser microscopy (TCS-SP2-AOBS; Leica, Mannheim Germany). The 543 and 633 nm lines of the He/Ne laser were used for the excitation of Mitotracker Red CMXRos and Alexa 633, respectively. Excitation of Hoechst 33258 was by UV laser.

Results and discussion

Generation of low-passage tumoral cell lines

Nine cell lines were established in primary cell culture directly from tumoral tissue specimens (Table 1). Phenotypic features were followed during the establishment of the cell lines. In most cultures we observed a first stage of crisis around passage 3–6, coinciding with the onset of senescent morphology in a percentage of cells. This percentage was not homogeneous and depended on the tumor sample. A few population doublings later, a second stage of crisis was observed in all the samples coinciding with a high degree of apoptosis within the cultures (Table 1). Once the cells passed this apoptotic stage, growth of the population resumed and cell culture became immortal. We also found that once this crisis stage passed, the specific phenotype of each cell line (Table 1) did not change during subsequent culture.

To avoid undesired alterations due to inherent tumor genetic instability in the newly generated cell lines, we amplified the cell lines to passage 14–16 and backups of the cultures were frozen. The experiments presented here were performed in cultures that did not exceed passage 18. However, small populations of each cell line

Table 1 Characteristics of the cell lines generated and used in this study

Cell line	Tumor origin	Observed crisis passage	Phenotype	Doubling time (h)
CNIO AA	leiomyosarcoma	7	epithelial	22
CNIO AB	bladder carcinoma	8	fibroblastic	57.1
CNIO AF	bladder carcinoma	8	fibroblastic	42.3
CNIO AH	melanoma metastasis	11	epithelial	18
CNIO AK	melanoma metastasis	11	epithelial	12.4
CNIO AL	epidermoid carcinoma	7	fibroblastic	24.4
CNIO AM	thyroid papillary carcinoma	12	epithelial	20.4
CNIO AS	uterine carcinoma	–	fibroblastic	42.5
CNIO AT	endometrium carcinoma	–	fibroblastic	32.2

were maintained in culture to ensure that they presented unrestricted proliferative capability.

The cell lines presented variable doubling times (Table 1). Among the cell lines generated, CNIO AH and AK derived from the same tumor sample, as did CNIO AB and AF. Both populations were identified and isolated on the basis of their different phenotype and the statistical differences in doubling time.

We have generated and characterized several tumor cell lines, and maintained these cell lines in low passage to approach the genetic conditions of the original tumors. Tumor cells undergo genetic changes in culture due to inherent genetic instability. To minimize the number of such alterations we generated low-passage tumor cell lines. A low-passage cell system from solid tumors, despite the necessary adaptation to culture, is the closest system to the original tumor for experimental investigation.

Characterization of the PI3K pathway

In order to determine the status of the PI3K pathway we first studied the presence of PTEN, p110α and p85α at both the mRNA and protein levels. We observed that all the cell lines express PTEN, p110α and p85α mRNAs (data not shown). We did not detect the transcript for p65α, the activating mutant of p85α (not shown). The study of protein levels showed that PTEN was only expressed in three cell lines (AB, AF and AS). PTEN protein was not detected in the rest of the cell lines (AA, AK, AH, AL, AM and AT) (Fig. 1A). Since PTEN usually disappears either due to mutations that alter the open reading frame or by methylation, we sequenced the mRNA from these cell lines and identified frameshift mutations (TT insertions) in the fifth exon. All the cell lines expressed p110α and p85α proteins (data not shown).

To study the status of the PI3K pathway in physiological conditions to determine constitutive activation, we checked AKT phosphorylation at Ser473 as the endpoint of the pathway. It has been reported that growth in low serum decreases the level of AKT phosphorylation, which can be sustained in the presence of activating alterations in the PI3K pathway [15]. We compared the level of AKT phosphorylation between cells cultured either in the presence of low serum or in 10% serum (standard conditions) for 24 h. We found that in most cell lines AKT phosphorylation is protected from serum deprivation (Fig. 1B), indicating the constitutive activation of PI3K. In AH and AK cell lines, serum depletion induced a decrease in the levels of AKT phosphorylation (Fig. 1B). Surprisingly, AH and AK cell lines do not express PTEN, which might indicate a constitutive activation of the pathway. We have used Ser473 phosphorylation as a measure of AKT activation. This residue is phosphorylated in the cells by a constitutively active kinase after PDKI has phosphorylated AKT at Thr308 (induced by PI3K activity or PTEN loss). Since AH and AK cell lines were from the same tumor sample, it is possible that the original tumor was defective in Ser473 kinase activity. Similar data were obtained with the phosphorylation status of FHKRL (data not shown), which is a direct target of active AKT [4,5]. No cell lines used in this study underwent apoptosis even after 72 h growing in low serum (data not shown).

To study the functional status of the PI3K pathway further we analyzed the levels of AKT phosphorylation after treatment with the PI3K inhibitor LY294002 for 1 h. Cells were cultured in 10% serum and LY294002 was added for 1 h at 10 μM final concentration. Under these conditions all the cell lines showed strong inhibition of AKT phosphorylation (Fig. 1C). It was interesting that the line AL showed a minimal reduction of AKT phosphorylation compared with the remaining cells lines. These data were confirmed by analyzing FKHRL phosphorylation under the same conditions (data not shown).

Response to PI3K inhibitor and gemcitabine

We measured the response of the different cell lines to PI3K inhibition. Cells were cultured and treated with different doses of LY294002 for 4 days. Medium was changed every day by adding fresh LY294002. In these conditions, we calculated the cytotoxic response to LY294002 (Table 2). All the cells showed an abrupt

Fig. 1

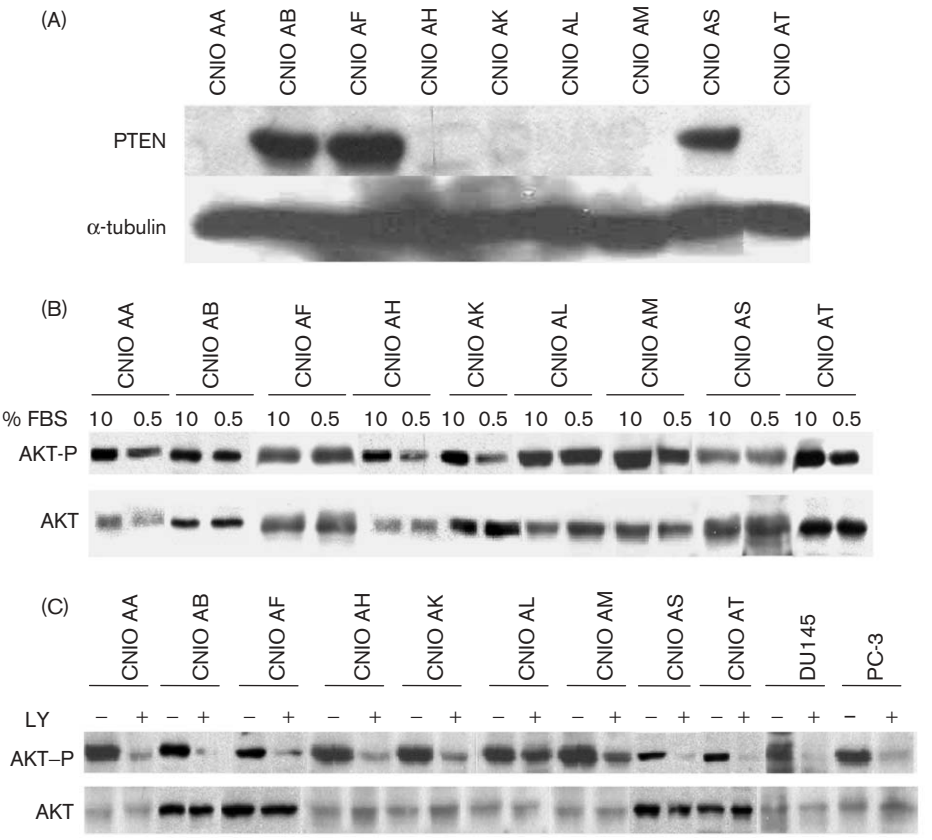

Characterization of the PI3K pathway in CNIO cell lines. (A) Immunoblot analysis of PTEN (B) Immunoblot analysis of phosphorylated AKT in total lysates from CNIO cell lines. Cells were grown to 80% confluence and starved for 24 h in 0.5% FBS or maintained in medium containing 10% FBS. Equal protein loading was evaluated by measuring the level of AKT. (C) Inhibition of AKT phosphorylation by the PI3K inhibitor LY294002. Immunoblot analysis of phosphorylated AKT in total lysates from CNIO cell lines treated with LY294002. Cells were grown to 80% confluence and treated with 10 μM LY294002 or vehicle (DMSO) for 1 h. Equal protein loading was evaluated by measuring the level of AKT. Lysates from DU145 and PC-3 were used as a negative and positive control, respectively, of constitutively activated PI3K pathway.

Table 2 IC_{50} and IC_{90} for LY294002 and gemcitabine in the different cell lines used in this study

Cell line	LY294002 (μM)		Gemcitabine (nM)	
	IC_{50}	IC_{90}	IC_{50}	IC_{90}
CNIO AA	6.9 ± 0.23	85 ± 2.85	0.6 ± 0.06	8 ± 0.7
CNIO AB	3.2 ± 0.36	70 ± 8	1.8 ± 0.17	14 ± 1.35
CNIO AF	6.9 ± 1.84	64 ± 17.07	5.3 ± 0.795	>100
CNIO AH	8.3 ± 1.4	100 ± 12	3.1 ± 1.02	60 ± 18
CNIO AK	8.0 ± 1.56	60 ± 11.7	2.0 ± 0.002	15 ± 0.15
CNIO AL	7.0 ± 0.64	61 ± 5.6	1.8 ± 0.13	12 ± 0.9
CNIO AM	8.8 ± 1.7	95 ± 19	2.8 ± 063	15 ± 3.4
CNIO AS	23.7 ± 0.23	>>100	20 ± 5.89	>100
CNIO AT	9.7 ± 0.97	>100	10.1 ± 2.8	>100

Cells were treated with different concentrations of drugs for 96 (LY294002) or 120 h (gemcitabine), and the concentration of drug resulting in 50 or 90% growth inhibition (IC_{50} or IC_{90}) calculated. See Materials and methods for details.

decrease in survival with IC_{50} for LY294002 below 10 μM. The only exception was the AS cell line, which showed higher resistance to LY294002 treatment (Table 2), whereas IC_{90} for LY294002 showed clear variations among the different cell lines. While most cell lines reach IC_{90} below 100 μM, the AS and AT cell lines showed more resistance to LY294002 treatment and did not reach IC_{90} below this dose.

We measured the response of the different cell lines to the treatment with gemcitabine – a cytotoxic drug that antagonizes nucleotide metabolism. Cells were cultured as before and treated with different doses of gemcitabine for 5 days. Medium with fresh gemcitabine was changed twice. In these conditions, we calculated the cytotoxic response to gemcitabine (Table 2). All the cells showed an abrupt decrease in survival, with an IC_{50} for gemcitabine below 10 nM. The only exception was the AS cell line that showed higher resistance to treatment (Table 2). As with the cytotoxic response to LY294002, AF, AS and AT cell lines showed higher resistance to gemcitabine treatment with IC_{90} not reached at the

assayed doses (100 nM). The AH cell line showed an intermediate behavior with IC_{90} reached at 60 nM.

Not all cell lines showed common resistance to both drugs; whereas AS, AT and AH cell lines showed resistance to both LY294002 and gemcitabine, AF cells showed resistance to gemcitabine, but not to LY294002. These data suggest that the mechanism of resistance to each drug may be at least partially independent.

Cooperation between LY294002 and gemcitabine

The PI3K pathway is important in protecting against apoptosis and has been strongly related to drug resistance [16]. To study whether the inhibition of the PI3K pathway has an effect on the response to cytotoxic stimuli, such as the drug gemcitabine, we measured the level of cooperation between inhibition of PI3K with LY294002 and the cytotoxic effect of gemcitabine.

To analyze the possible cooperation between both drugs, cells were treated with different doses of gemcitabine and LY294002. To determine a possible cooperation, the dose–response curve of gemcitabine alone was compared with the dose–response curve obtained in cells simultaneously treated with gemcitabine and different concentrations of LY294002. The cooperative index (RI) was obtained by applying Kern's method [13] as described in Materials and methods. We consider that synergism exists between two drugs if $RI > 1$ and synergism is pharmacologically relevant if $RI > 2$ [14].

We found that LY294002 cooperated with gemcitabine, strongly reducing gemcitabine IC_{50} (not shown) for most cell lines. The analysis of the cooperative index (Table 3) shows pharmacologically relevant synergism of both drugs at suboptimal doses in half of the cell lines. Additive effects were found in AF and AM cell lines, although no cooperative or additive effects were found in AS and AT cell lines.

Table 3 Cooperation between LY294002 and gemcitabine

Gemcitabine (nM)	Cooperative index (RI) for 1 μM LY294002								
	AK	AA	AL	AH	AB	AM	AF	AS	AT
0.1	7.2	4.4	9.1	1.2	2.4	1.3	1.1	0.9	1.1
1	10.2	6.0	23.1	2.9	2.7	1.4	1.1	0.8	0.9
10	2.7	2.3	7.3	1.5	2.1	2.2	0.6	1.0	1.1
100	3.3	2.5	7.2	1.4	1.8	1.8	0.7	1.1	1.1

Cells were treated with different doses of gemcitabine and LY294002. To determine a possible cooperation, the dose–response curve of gemcitabine alone was compared with the dose–response curve obtained in cells simultaneously treated with gemcitabine and different concentrations of LY294002. The cooperative index was obtained by applying Kern's method subsequently modified by Romanelli (see Materials and methods for details). We consider that synergism exists between two drugs if $RI > 1$ and this synergism is pharmacologically relevant when $RI > 2$.

Molecular determinants of LY294002 and gemcitabine synergism

To gain insight into the molecules that might play a role in the synergism, we focused on proteins that carry out a relevant function in the response to both drugs.

The presence of p73 has been reported as relevant to sensitivity to cisplatin [17] and other cytotoxic drugs [18,19]. As p73 can regulate transcription of pro-apoptotic genes in response to different DNA-damaging agents, and consequently be responsible for the behavior of the cell lines against these agents, we also investigated the presence of p73α in our cell lines. Using RT-PCR, we detected the p73α transcript in five cell lines (AA, AH, AK, AL and AM); p73α was absent in the remaining cell lines (Fig. 2A).

As cells can respond to DNA damage and other cytotoxic drugs in a p53-dependent manner, we also checked the status of p53 in our cell lines. We analyzed the presence of mutant p53 (Fig. 2B) by examining p53 levels. Wild-type p53 levels are commonly undetectable by Western blot due to the high turnover of the protein that maintains wild-type p53 at very low levels [20]. Inactivating mutations in p53 commonly impair its degradation, therefore leading to the accumulation of the p53 protein in the cell that can now be detected by Western blot. We found that the lines AA, AH, AK, AL and AM carry mutant p53 protein, while in the other lines this was not detected (Fig. 2B). We confirmed these data by sequencing the p53 transcript in all cell lines. We have found that AA, AH, AK, AL and AM carry the 273H inactivating mutation of p53, whereas the rest only express wild-type transcripts (data not shown). We found a mutual exclusion between p53 wild-type and the presence of p73. Cell lines carrying mutated p53 expressed the p73 transcript, whereas in cells with wild-type p53, the p73 transcript is lost. In cell lines with mutated p53, p73 could therefore be the main regulator of the apoptotic response to cytotoxic drugs.

It has been previously observed that Bax plays an important role in the regulation of apoptosis induced by chemotherapeutic agents such as gemcitabine [21]. Bax expression might respond to either p53 or p73 activation [22,23]. We measured the basal levels of Bax in our low-passage cell lines and found that lines with p53 wild-type, AB, AS and AT, showed higher levels of Bax protein (Fig. 2B). These high levels of Bax correlated with normal levels of Bcl-X_L (Fig. 2B), an anti-apoptotic partner of Bax that might inhibit its function [24,25]. Only AA and AH showed higher levels of Bcl-X_L.

Moreover, Bax is phosphorylated, preventing its pro-apoptotic function by activated AKT [5]. We measured the levels of Bax and Bcl-X_L in response to treatments,

Fig. 2

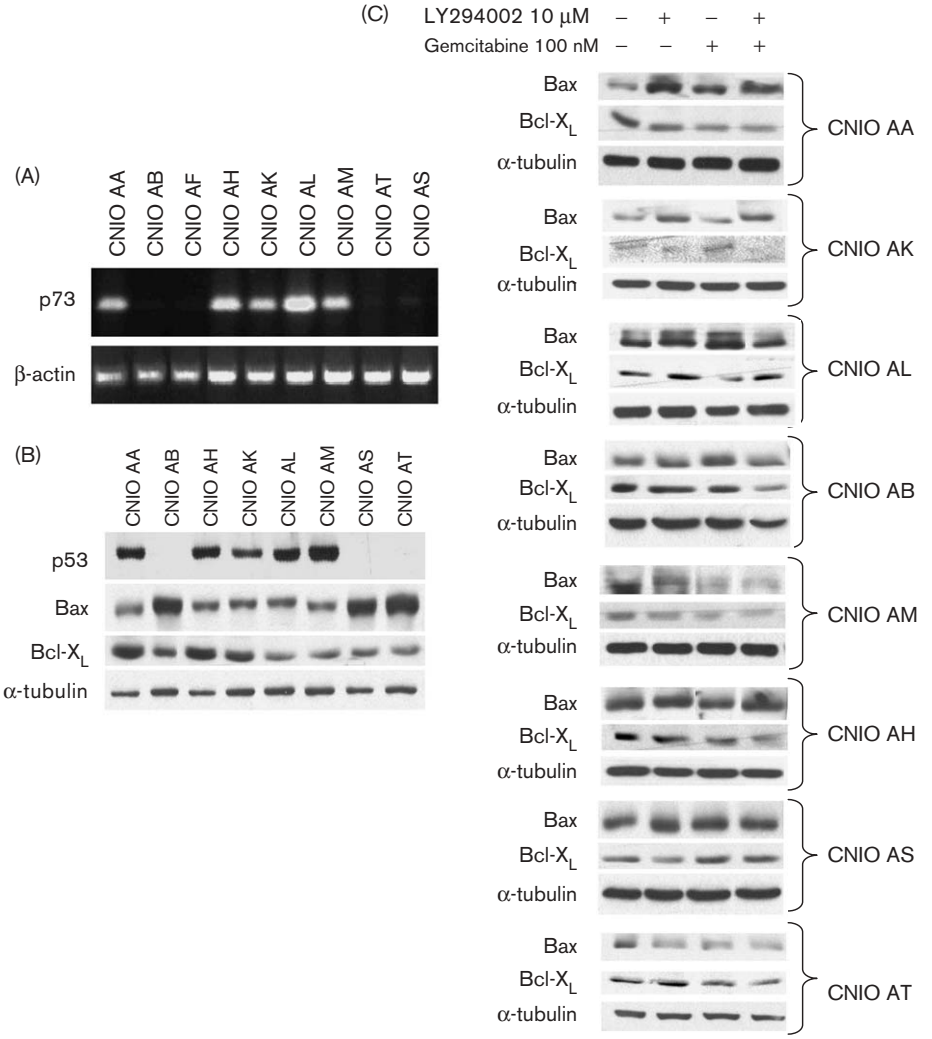

Molecular determinants of LY294002 and gemcitabine synergism. (A) RT-PCR of p73α. (B) Immunoblot analysis of p53, Bax and Bcl-X_L in total lysates from CNIO cell lines. Whole-cell lysates (5 μg) from cells grown at 80% confluence were isolated and analyzed by immunoblotting with polyclonal anti-p53, anti Bax or anti Bcl-X_L antibodies. α-Tubulin was used as loading control. (C) Bax induction upon LY294002 and gemcitabine treatment. Immunoblot analysis of Bax and Bcl-X_L in total lysates from CNIO cell lines. Cells were grown to 80% confluence and treated with 10 μM LY294002, 100 nM gemcitabine, a combination of both drugs or vehicle (DMSO) for 24 h. Equal protein loading was evaluated by measuring the level of α-tubulin.

i.e. LY294002, gemcitabine or both. Cell lines AA, AL, AK and AB treated with LY294002 showed an increase in Bax protein that was maintained in the presence of gemcitabine (Fig. 2C). We also observed an increase of Bax by gemcitabine treatment in the AB cell line. No increase was detected in AM, AH, AS and AT. In parallel, a clear decrease in Bcl-X_L was observed in AA, AK, AH, AB and AM. No decrease was observed in AL, AT and AS (Fig. 2C). These results seem to indicate that the balance between Bax and Bcl-X_L levels might trigger the apoptosis induced by PI3K inhibition, and might be responsible for the synergism observed between LY294002 and gemcitabine.

PI3K inhibition by LY294002 should increase the translocation of Bax to the mitochondria, increasing the apoptotic loading of the cells. To gain insight into the implication of Bax in the sensitivity of our cell lines to LY294002 and gemcitabine, we measured Bax protein translocation to the mitochondria. Cells were treated with 10 μM LY294002 or 100 nM gemcitabine, or with a combination of the two, for 24 h. Cells were then fixed and stained for Bax or a mitochondrial marker, and localization of Bax was analyzed using confocal microscopy (Fig. 3).

Cell line AB that showed synergism, demonstrated high levels of Bax distributed both in the nucleus and

Fig. 3

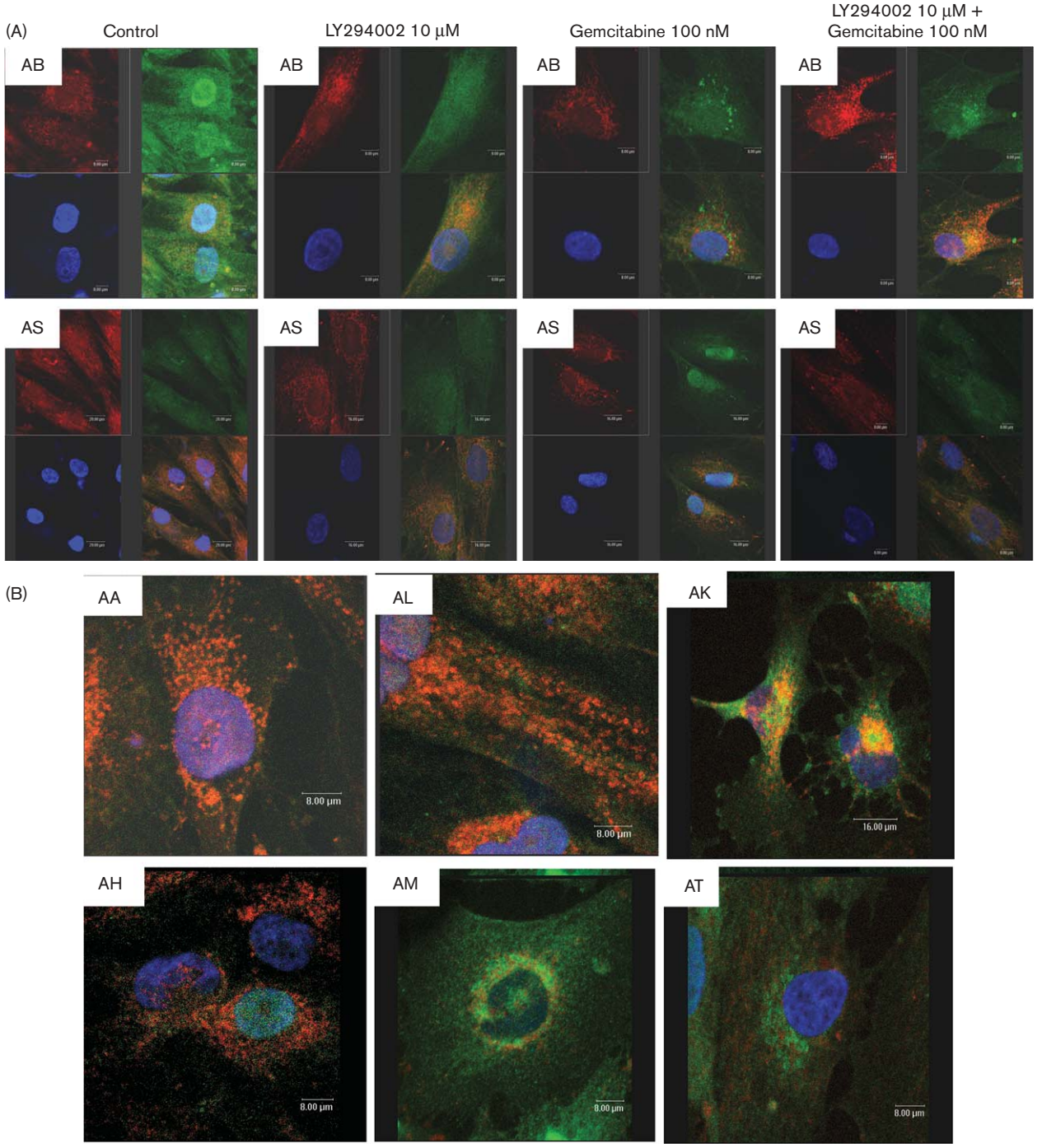

Mitochondrial translocation of Bax. CNIO cell lines were treated with 10 μM LY294002, 100 nM gemcitabine, a combination of both drugs or vehicle (DMSO) for 24 h. The localization of Bax was determined by fluorescence under confocal microscopy as described in Materials and methods. (A) Immunofluorescence of CNIO AB and AS cells is shown before and after drug treatments. For each treatment, the left upper picture shows Mitotracker staining – a fluorescent probe that specifically stains mitochondria in red; on the right upper picture, Bax is shown in green; on the left lower picture, the nucleus is shown in blue; and a merged image is shown on the right lower picture. (B) Merged images of staining for Bax, mitochondria and the nucleus of CNIO cell lines.

cytoplasm. LY294002 and gemcitabine treatments localize part of the Bax in the mitochondria (Fig. 3A). Combined treatment localized most Bax in the mitochondria, explaining the synergistic effects of both treatments. In the AS cell line, showing no cooperation, Bax is also uniformly distributed; however, treatment

with the drugs does not localize Bax in the mitochondria (Fig. 3A). Similar correlations were found in the remaining cell lines (Fig. 3B). AA, AL and AK cell lines showed localization of Bax in the mitochondria after combined treatment with LY294002 and gemcitabine. However, AM, AH and AT, which did not show a synergistic effect, do not demonstrate mitochondrial localization of Bax after combined treatments either (Fig. 3B).

It has been shown that activated AKT can phosphorylate the pro-apoptotic proteins Bad and Bax, hampering their ability to heterodimerize with Bcl-2 or Bcl-X_L, and resulting in the suppression of apoptosis [26]. Moreover, the PI3K pathway also contributes to cell survival through other mechanisms such as phosphorylation of caspase-9, GSK3, p21, p27, p70S6K or LKB, all of them involved in the regulation of apoptosis [27]. Therefore, it seems reasonable to speculate that inhibition of PI3K and subsequent inhibition of AKT would promote apoptosis. The PI3K inhibitor LY249002 blocks AKT and FKHRL-1 phosphorylation, and continuous treatment of the cells with this PI3K inhibitor leads to cell death with an IC_{50} in the low micromolar range. However, significant differences among IC_{90}s were observed among the different cell lines (Table 2). In our experience these differences are not due to mutations that activate the pathway since all the cell lines show constitutive PI3K activation. Although LY294002 specifically inhibits PI3K at the concentrations used in this study, it has also been shown to inhibit other enzymes [28,29]. Therefore, it is possible that the effects of LY294002 are due, at least in part, to those other enzymes and their alterations are responsible for the observed differences in cytotoxicity.

Our cell lines show sensitivity to gemcitabine with an IC_{50} in the low nanomolar range. However, very significant differences on IC_{90}s were detected among the different cell lines (Table 3). These differences may be due to alterations in the Bax:Bcl-X_L ratio after gemcitabine treatment, since the most sensitive cell lines AA, AK and AL showed induction of Bax and reduction of Bcl-X_L levels. Furthermore, AS and AT cell lines showed greater resistance to gemcitabine, correlating with no induction of Bax and no reduction of Bcl-X_L protein levels. This explanation would correlate well with the available literature. Is has been shown that overexpression of Bax sensitizes human pancreatic cells to apoptosis induced by gemcitabine [21]. However, E2F1 in combination with gemcitabine is capable of efficiently killing pancreatic tumoral cells. This therapeutic effect directly correlates with the induction of the p53 homolog p73 [30], and it has been recently demonstrated that p73 can elicit apoptosis via the mitochondrial pathway using PUMA and Bax as mediators [31].

LY294002 enhanced apoptosis caused by doxorubicin, trastuzumab, etoposide, tamoxifen or paclitaxel with cell line specificity [16,32–35]. Thus, approaches inhibiting the PI3K pathway may be of use when combined with traditional forms of chemotherapy. Previously, LY294002 was shown to enhance gemcitabine-induced apoptosis in a small number of pancreatic cell lines [34], but the study did not address the activation status of the PI3K pathway nor the molecular determinants of cooperation. In contrast, other authors have shown that the AKT/PI3K pathway is not involved in gemcitabine resistance of pancreatic carcinoma cell lines and gemcitabine-induced cell death is not enhanced by treatment with LY294002 [36]. Since our cell lines are more sensitive to gemcitabine, it is possible that only when the cells show sensitivity to gemcitabine we could expect synergism with LY294002. Our study characterizes the constitutive activation of PI3K pathway in low-passage tumor cell lines. Moreover, we show that LY294002 treatment at the doses used in this study leads to PI3K inhibition. These lines also respond to gemcitabine treatment. We also found a pharmacologically relevant synergism between LY294002 and gemcitabine at suboptimal doses in most cell lines (Table 3). Among all the cell lines tested, in AS, AM, AF and AT cells treatment with LY294002 did not synergize with gemcitabine, although additive effects were found in AM and AF, these cells lines being the least sensitive to gemcitabine, which support our previous hypothesis.

We have explored some molecular determinants that could explain this pharmacological cooperation. We have focused on Bax, since it has been shown that activated AKT can phosphorylate the pro-apoptotic Bcl-2 family member Bax at Ser184, inhibiting its conformational change and its subsequent translocation to mitochondria, thus preventing Bif-1 binding to Bax and alterations in mitochondrial membrane potential, cytochrome *c* release, caspase activation, and apoptosis [37,38]. Furthermore, Bcl-X_L levels can be regulated by PI3K pathway, and upregulation of this protein implies survival and downregulation leads to apoptosis. Thrombopoietin-induced survival of megakaryocytic cells is regulated by the PI3K pathway in cooperation with other pathways via Bcl-X_L expression [39]. The induction of apoptosis by indol-3-carbinol was partly because of the inhibition of AKT activation, and downregulation of BAD and Bcl-X_L [40]; the inhibition of AKT is implicated in apoptosis induced by oxysterol allowing the activation of Bim and Bad, and down-regulating the levels of Bcl-X_L as well [41].

In our cells, pharmacological synergism between LY294002 and gemcitabine is accompanied by a change in the Bax:Bcl-X_L ratio and Bax localization to the mitochondria. We observed an increase in Bax levels and a reduction in Bcl-X_L levels in cells where a

synergistic effect could be found. However, no similar behavior could be found in the other cell lines. In the presence of PI3K inhibitors, Bax will remain unphosphorylated, allowing its translocation to the mitochondrial membrane. However, in the cells where no synergistic effects were found, the Bax:Bcl-X_L ratio remains largely unaltered, inhibiting the synergistic effect induced by PI3K inhibition. The increase in the Bax:Bcl-X_L ratio is accompanied by the absence of Bax phosphorylation, due to PI3K inhibition, allowing its translocation to the mitochondrial membrane and forwarding synergistic induction of apoptosis. The maintenance of the Bax:Bcl-X_L ratio in cell lines despite unphosphorylation of Bax does not induce a synergistic effect, maintaining similar or additive effects in the induction of apoptosis.

Cooperation between the apoptotic load induced by DNA damage and inhibition of the survival pathway PI3K implies an increase of the apoptotic response of the cells, and this would be a general mechanism rather than cell specific given that our primary cell lines are from different origins.

The characterization of our low-passage cell lines indicates that, through different mechanisms, most of them have a constitutively activated PI3K pathway, therefore suggesting that the PI3K pathway might constitute a suitable target for cancer therapy. Our data support previous work indicating that PI3K inhibition might help classical chemotherapeutic treatments and that the strengthening of suboptimal doses might be effective for these purposes of decreasing the risk of side-effects. We have found that for this synergism to occur cells have to be able to be induced to death by increased apoptotic loading, such as Bax induction or Bcl-X_L downregulation.

The identification of possible molecular determinants of synergisms could help to identify suitable receptors of combined treatments, thus decreasing undesired side-effects.

Acknowledgements

Tissue samples used to generate cell lines were provided by the CNIO Spanish National Tissue Bank Network. The authors wish to thank other members of the CNIO Assay Development Group, Jose A. Carrodeguas and Amanda Wren for helpful comments and critical reading of this manuscript, and also the CNIO Confocal Microscopy Unit for helping with the interpretation of the images.

References

1 Cantley LC, Neel BG. New insights into tumor suppression: PTEN suppresses tumor formation by restraining the phosphoinositide 3-kinase/AKT pathway. *Proc Natl Acad Sci USA* 1999; **96**:4240–4245.
2 Kodaki T, Woscholski R, Hallberg B, Rodriguez-Viciana P, Downward J, Parker PJ. The activation of phosphatidylinositol 3-kinase by Ras. *Curr Biol* 1994; **4**:798–806.
3 Rodriguez-Viciana P, Warne PH, Dhand R, Vanhaesebroeck B, Gout I, Fry MJ, *et al.* Phosphatidylinositol-3-OH kinase as a direct target of Ras. *Nature* 1994; **370**:527–532.
4 Osaki M, Oshimura M, Ito H. PI3K–Akt pathway: its functions and alterations in human cancer. *Apoptosis* 2004; **9**:667–676.
5 Kim D, Dan HC, Park S, Yang L, Liu Q, Kaneko S, *et al.* AKT/PKB signaling mechanisms in cancer and chemoresistance. *Front Biosci* 2005; **10**:975–987.
6 Sansal I, Sellers WR. The biology and clinical relevance of the PTEN tumor suppressor pathway. *J Clin Oncol* 2004; **22**:2954–2963.
7 Eves EM, Xiong W, Bellacosa A, Kennedy SG, Tsichlis PN, Rosner MR, *et al.* Akt, a target of phosphatidylinositol 3-kinase, inhibits apoptosis in a differentiating neuronal cell line. *Mol Cell Biol* 1998; **18**:2143–2152.
8 Link W, Rosado A, Fominaya J, Thomas JE, Carnero A. Membrane localization of all class I PI 3-kinase isoforms suppresses c-Myc-induced apoptosis in Rat1 fibroblasts via Akt. *J Cell Biochem* 2005; **95**:979–989.
9 Haas-Kogan D, Shalev N, Wong M, Mills G, Yount G, Stokoe D. Protein kinase B (PKB/Akt) activity is elevated in glioblastoma cells due to mutation of the tumor suppressor PTEN/MMAC. *Curr Biol* 1998; **8**:1195–1198.
10 Nesterov A, Lu X, Johnson M, Miller GJ, Ivashchenko Y, Kraft AS. Elevated AKT activity protects the prostate cancer cell line LNCaP from TRAIL-induced apoptosis. *J Biol Chem* 2001; **276**:10767–10774.
11 Lu Y, Lin YZ, LaPushin R, Cuevas B, Fang X, Yu SX, *et al.* The PTEN/MMAC1/TEP tumor suppressor gene decreases cell growth and induces apoptosis and anoikis in breast cancer cells. *Oncogene* 1999; **18**:7034–7045.
12 Shayesteh L, Lu Y, Kuo WL, Baldocchi R, Godfrey T, Collins C, *et al.* PIK3CA is implicated as an oncogene in ovarian cancer. *Nat Genet* 1999; **21**:99–102.
13 Kern DH, Morgan CR, Hildebrand-Zanki SU. *In vitro* pharmacodynamics of 1-beta-D-arabinofuranosylcytosine: synergy of antitumor activity with *cis*-diamminedichloroplatinum(II). *Cancer Res* 1988; **48**:117–121.
14 Romanelli S, Perego P, Pratesi G, Carenini N, Tortoreto M, Zunino F. *In vitro* and *in vivo* interaction between cisplatin and topotecan in ovarian carcinoma systems. *Cancer Chemother Pharmacol* 1998; **41**:385–390.
15 Andjelkovic M, Jakubowicz T, Cron P, Ming XF, Han JW, Hemmings BA. Activation and phosphorylation of a pleckstrin homology domain containing protein kinase (RAC-PK/PKB) promoted by serum and protein phosphatase inhibitors. *Proc Natl Acad Sci USA* 1996; **93**:5699–5704.
16 Brognard J, Clark AS, Ni Y, Dennis PA. Akt/protein kinase B is constitutively active in non-small cell lung cancer cells and promotes cellular survival and resistance to chemotherapy and radiation. *Cancer Res* 2001; **61**:3986–3997.
17 Gong JG, Costanzo A, Yang HQ, Melino G, Kaelin WG Jr, Levrero M, *et al.* The tyrosine kinase c-Abl regulates p73 in apoptotic response to cisplatin-induced DNA damage. *Nature* 1999; **399**:806–809.
18 Costanzo A, Merlo P, Pediconi N, Fulco M, Sartorelli V, Cole PA, *et al.* DNA damage-dependent acetylation of p73 dictates the selective activation of apoptotic target genes. *Mol Cell* 2002; **9**:175–186.
19 Irwin MS, Kondo K, Marin MC, Cheng LS, Hahn WC, Kaelin WG Jr. Chemosensitivity linked to p73 function. *Cancer Cell* 2003; **3**:403–410.
20 Blagosklonny MV. p53 from complexity to simplicity: mutant p53 stabilization, gain-of-function, and dominant-negative effect. *FASEB J* 2000; **14**:1901–1907.
21 Xu ZW, Friess H, Buchler MW, Solioz M. Overexpression of Bax sensitizes human pancreatic cancer cells to apoptosis induced by chemotherapeutic agents. *Cancer Chemother Pharmacol* 2002; **49**:504–510.
22 Miyashita T, Reed JC. Tumor suppressor p53 is a direct transcriptional activator of the human *bax* gene. *Cell* 1995; **80**:293–299.
23 Zhu J, Jiang J, Zhou W, Chen X. The potential tumor suppressor p73 differentially regulates cellular p53 target genes. *Cancer Res* 1998; **58**:5061–5065.
24 Gross A, Jockel J, Wei MC, Korsmeyer SJ. Enforced dimerization of BAX results in its translocation, mitochondrial dysfunction and apoptosis. *EMBO J* 1998; **17**:3878–3885.
25 Decaudin D, Geley S, Hirsch T, Castedo M, Marchetti P, Macho A, *et al.* Bcl-2 and Bcl-X_L antagonize the mitochondrial dysfunction preceding nuclear apoptosis induced by chemotherapeutic agents. *Cancer Res* 1997; **57**:62–67.
26 Kirkin V, Joos S, Zornig M. The role of Bcl-2 family members in tumorigenesis. *Biochim Biophys Acta* 2004; **1644**:229–249.
27 Susin SA, Zamzami N, Kroemer G. Mitochondria as regulators of apoptosis: doubt no more. *Biochim Biophys Acta* 1998; **1366**:151–165.

28 Davies SP, Reddy H, Caivano M, Cohen P. Specificity and mechanism of action of some commonly used protein kinase inhibitors. *Biochem J* 2000; **351**:95–105.
29 Stein RC. Prospects for phosphoinositide 3-kinase inhibition as a cancer treatment. *Endocr Relat Cancer* 2001; **8**:237–248.
30 Rodicker F, Stiewe T, Zimmermann S, Putzer BM. Therapeutic efficacy of E2F1 in pancreatic cancer correlates with TP73 induction. *Cancer Res* 2001; **61**:7052–7055.
31 Melino G, Bernassola F, Ranalli M, Yee K, Zong WX, Corazzari M, *et al.* p73 Induces apoptosis via PUMA transactivation and Bax mitochondrial translocation. *J Biol Chem* 2004; **279**:8076–8083.
32 Shingu T, Yamada K, Hara N, Moritake K, Osago H, Terashima M, *et al.* Synergistic augmentation of antimicrotubule agent-induced cytotoxicity by a phosphoinositide 3-kinase inhibitor in human malignant glioma cells. *Cancer Res* 2003; **63**:4044–4047.
33 Hu L, Hofmann J, Lu Y, Mills GB, Jaffe RB. Inhibition of phosphatidylinositol 3′-kinase increases efficacy of paclitaxel in *in vitro* and *in vivo* ovarian cancer models. *Cancer Res* 2002; **62**:1087–1092.
34 Ng SSW, Tsao MS, Chow S, Hedley DW. Inhibition of phosphatidylinositide 3-kinase enhances gemcitabine-induced apoptosis in human pancreatic cancer cells. *Cancer Res* 2000; **60**:5451–5455.
35 Krystal GW, Sulanke G, Litz J. Inhibition of phosphatidylinositol 3-kinase–Akt signaling blocks growth, promotes apoptosis, and enhances sensitivity of small cell lung cancer cells to chemotherapy. *Mol Cancer Ther* 2002; **1**:913–922.
36 Arlt A, Gehrz A, Muerkoster S, Vorndamm J, Kruse ML, Folsch UR, *et al.* Role of NF-kappaB and Akt/PI3K in the resistance of pancreatic carcinoma cell lines against gemcitabine-induced cell death. *Oncogene* 2003; **22**: 3243–3251.
37 Yamaguchi H, Wang HG. The protein kinase PKB/Akt regulates cell survival and apoptosis by inhibiting Bax conformational change. *Oncogene* 2001; **20**:7779–7786.
38 Tsuruta F, Masuyama N, Gotoh Y. The phosphatidylinositol 3-kinase (PI3K)–Akt pathway suppresses Bax translocation to mitochondria. *J Biol Chem* 2002; **277**:14040–14047.
39 Kirito K, Watanabe T, Sawada K, Endo H, Ozawa K, Komatsu N. Thrombopoietin regulates Bcl-xL gene expression through Stat5 and phosphatidylinositol 3-kinase activation pathways. *J Biol Chem* 2002; **277**:8329–8337.
40 Chinni SR, Sarkar FH. Akt inactivation is a key event in indole-3-carbinol-induced apoptosis in PC-3 cells. *Clin Cancer Res* 2002; **8**:1228–1236.
41 Rusinol AE, Thewke D, Liu J, Freeman N, Panini SR, Sinensky MS. AKT/protein kinase B regulation of BCL family members during oxysterol-induced apoptosis. *J Biol Chem* 2004; **279**:1392–1399.